sustainability

MDPI

Brief Report

Effect of Humic Acid Binder on the Preparation of Oxidized Pellets from Vanadium-Bearing Titanomagnetite Concentrate

Guanghui Li [1], Yongkang Zhang [1,2], Xin Zhang [1], Feiyu Meng [1,2], Pengxu Cao [1] and Lingyun Yi [1,*]

[1] School of Minerals Processing and Bioengineering, Central South University, Changsha 410083, China; liguangh@csu.edu.cn (G.L.); 185601018@csu.edu.cn (Y.Z.); zhangxinnv@csu.edu.cn (X.Z.); meiyu1616585@163.com (F.M.); caopengx@csu.edu.cn (P.C.)
[2] Pelletizing Plant of Panzhihua Gangcheng Group Co., Ltd., Panzhihua 617000, China
* Correspondence: ylycsu@126.com

Abstract: In order to pursue the goal of low-carbon ironmaking, a new type of humic acid (HA)-based binder was applied to the preparation of oxidized pellets from vanadium-bearing titanomagnetite (VTM) in this work. Effects of the HA binder (or with limestone) on the balling, preheating, and roasting behaviors of VTM were comparatively studied with bentonite. The embedded features of each mineral phase in sintered pellets, especially the crystallization and growth state of hematite grains, were deeply investigated by XRD, optical microscopy, and SEM–EDS measures. The binder dosage can be cut down by 50% when HA was used instead of bentonite. Fine hematite grains in HA pellets evolved into plump interlocking grains with ~5% of limestone addition. Pseudobrookite and magnesioferrite spinel phase formed at the optimal sintering temperature of 1250 °C, which could hinder the crystallization of hematite and affect the strength of final pellets.

Keywords: humic acid binder; vanadium-bearing titanomagnetite; oxidized pellets preparation; crystallization of hematite grains; embedding features of mineral phase

Citation: Li, G.; Zhang, Y.; Zhang, X.; Meng, F.; Cao, P.; Yi, L. Effect of Humic Acid Binder on the Preparation of Oxidized Pellets from Vanadium-Bearing Titanomagnetite Concentrate. *Sustainability* **2023**, *15*, 6454. https://doi.org/10.3390/su15086454

Academic Editor: Gujie Qian

Received: 6 March 2023
Revised: 4 April 2023
Accepted: 8 April 2023
Published: 11 April 2023

1. Introduction

Under the background of carbon peak and neutrality goals, how to achieve carbon emission reduction has become the focus in China's steel industry. Replacing the high proportion of sinter by the pellets with better smelting performance but less pollution for blast furnace operation is considered to be one of the important ways [1,2]. In 2022, China's total pellet production reached 230 million tons, with new production capacity of 8 million tons. According to the plan of steel industry, the proportion of pellet use will be increased from the current 17% to about 30% in the next five years, corresponding to carbon emission reduction of 40 million tons [3].

Binder is an important auxiliary raw material for oxidized pellets production, and its performance directly determines the quality of pellets. At present, bentonite is commonly used as binder in most domestic pellet plants. The dosage is always within 1.5%~2.0%, sometimes higher than 3.0%, which is much higher than the average level (0.6%~0.8%) of pellets from abroad [4,5]. Bentonite use inevitably reduces the iron grade of pellets, thereby increasing fuel consumption of the blast furnace [6]. Organic binders have been developed to avoid this defect. Organic binders can be burnt out during the high temperature roasting process with almost no residue left, which would not affect the iron grade of pellets [6,7]. However, the use of organic binder always brings about strength drop on sintered pellets, due to the higher porosity and less bonding phase between the iron oxide particles [8,9]. Based on this, a HA binder (a new type of binder composed of organic and inorganic components) was invented by our research group. It has the advantages of both high bonding properties and low residue, and, thus, has good application prospects in the production of iron ore pellets [10–12].

As a typical polymetallic ore in China, vanadium-bearing titanomagnetite (VTM), with a relatively low iron grade (57%~60%), is always difficult to process. To make its oxidized pellets always requires more bentonite, higher temperatures, and a longer duration compared to that of ordinary magnetite concentrates [13,14]. Therefore, applying the HA composite binder to VTM pelletizing is of great significance for the upgrading of VTM pellet production. This work studied the effects of HA binder on the balling, preheating, and roasting behaviors of VTM systematically by comparing them with bentonite. The morphology evolution and interaction features of the mineral phases during high temperature processes were deeply investigated by XRD, optical microscopy, and SEM–EDS measures to explain the induration mechanism of VTM-oxidized pellets.

2. Experimental Materials and Method

2.1. Materials

The compositions of vanadium-bearing titanomagnetite, bentonite, and limestone used in this work are given in Table 1. The VTM concentrated with natural basicity (CaO/SiO_2) of 0.17 was mainly composed of 55.45% total iron and 11.17% TiO_2. The bentonite with 59.66% of SiO_2, 12.43% of Al_2O_3, and 2.68% of Na_2O was a typical sodium-based bentonite. Limestone with 49.92% of CaO and 2.21% of MgO was used as an additive for basicity regulation of oxidized pellets.

Table 1. Chemical composition of VTM concentrate and bentonite/wt%.

Component	Fe Total	FeO	TiO_2	V_2O_5	SiO_2	CaO	MgO	Al_2O_3	K_2O	Na_2O	LOI
VTM	55.45	32.36	11.17	0.61	4.39	0.75	3.16	3.05	0.02	0.11	−1.33
Bentonite	-	-	-	-	59.66	4.60	3.40	12.43	0.94	2.68	14.08
Limestone	-	-	-	-	2.35	49.92	2.21	0.37	0.11	0.05	42.77

VTM was identified as a titanomagnetite concentrate with minor traces of ilmenite and trace of hortonolite, based on the XRD pattern (Figure 1a). The SEM image (Figure 1b) shows that the VTM has irregular particles with size distributed between 10~100 μm. The coarse particles are mostly magnetite (white) and gangue (light gray), while the fine particles are almost entirely pure magnetite.

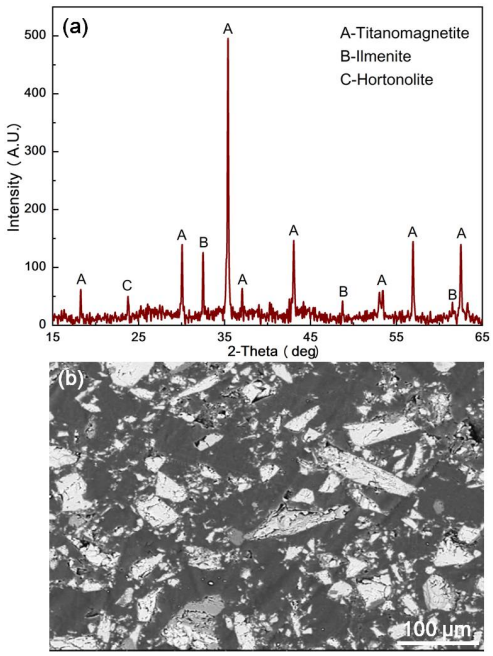

Figure 1. XRD pattern (**a**) and SEM image (**b**) of VTM.

The particle size distribution of the VTM concentrate, bentonite, and limestone are shown in Figure 2. The VTM with D_{50} of 35.22 µm is a suitable raw material for pellet-making. A raw material containing the appropriate amount of fine particles can improve the strength of green balls and the consolidation of pellets. For the bentonite and limestone with similar particle size distribution, their D_{50} reaches as fine as 7.75 µm and 6.75 µm, respectively. In general, fine particle size facilitates the dispersion and mixing of additives (bentonite and limestone) in VTM concentrate and, therefore, its pelletizing process.

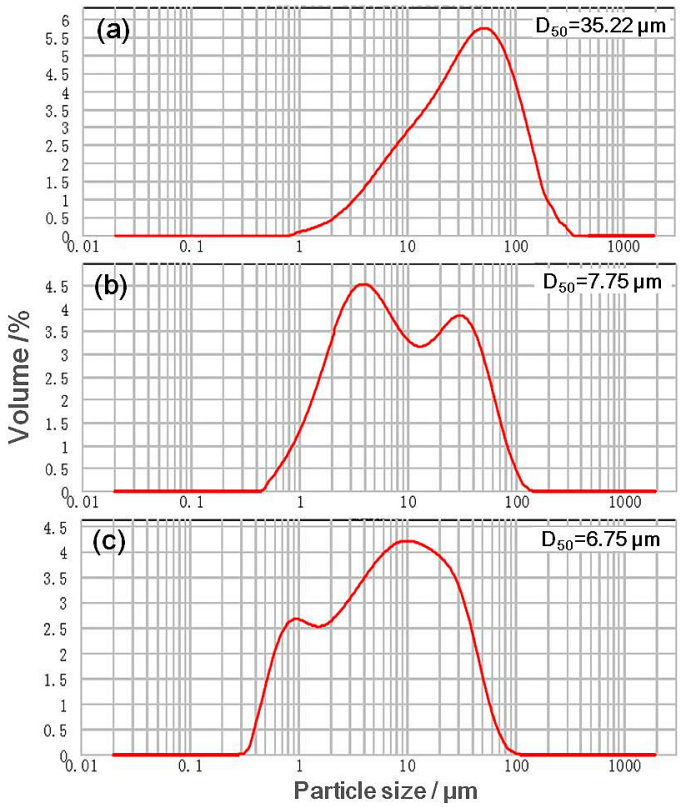

Figure 2. Particle size distribution of VTM concentrate (**a**), bentonite (**b**), and limestone (**c**).

Proximate analysis of the HA-based binder used in this work and the chemical composition of HA binder ash are shown in Table 2. The moisture, volatiles, and fixed carbon of the HA binder are 15.62%, 18.21% and 26.66%, respectively, which is burnt out during the pellet-sintering process. About 39.51% of ash could remain in sintered pellets, which are mainly composed of 56.90% of SiO_2, 24.69% of Al_2O_3, and 6.80% of Na_2O.

Table 2. Proximate analysis (ad) of HA binder and chemical composition of binder ash/wt%.

Component	Moisture	Volatiles	Ash	Fixed Carbon	Chemical Composition of Ash					
					Fe_2O_3	SiO_2	CaO	MgO	Al_2O_3	Na_2O
Mass/wt%	15.62	18.21	39.51	26.66	5.86	56.90	0.58	0.70	24.69	6.80

ad: air-dried basis.

2.2. Method

Balling: VTM concentrate were fully mixed with a certain amount of bentonite, HA binder, or limestone. The mixture was pelletized to green balls by a disc pelletizer (Φ 1 m, with dip angle of 45° and rotation speed of 23 rpm) in 10~12 min with moisture of ~8.0%. Then, the drop strength, compressive strength, and decrepitation temperature of the green balls (size: 10~16 mm) were tested [8,15].

Sintering: To simulate the thermal regulation of industrial grate–kiln roasting process, pellets were sintered in two stages in an experimental tube furnace: (1) preheating, dried green balls were roasted at 900~1000 °C for 12~18 min; (2) oxidized roasting, the preheated pellets were roasted at 1200~1300 °C for 8~12 min. Then, the compressive strength of the sintered pellets was measured with a universal material testing machine (KL-WS) as they cooled to room temperature.

Characterization: The mineral phase composition of the oxidized pellet was identified by X-ray diffraction (Rigaku, Japan, D/max2500). Morphology and dissemination features of minerals in oxidized pellets were observed by optical microscopy (Leica, Germany, DMRXP) and scanning electron microscope (FEI, Netherlands, Quanta-200) equipped with EDS.

3. Results and Discussion

3.1. Effect of HA Binder on Balling Characteristic

Figure 3 displays the properties of the green balls as bentonite, HA binder, and limestone were blended. Generally, green balls with drop strength > 3 times/0.5 m, compressive strength > 10 N/pellet, and decrepitation temperature > 400 °C are considered qualified for the subsequent sintering process [15].

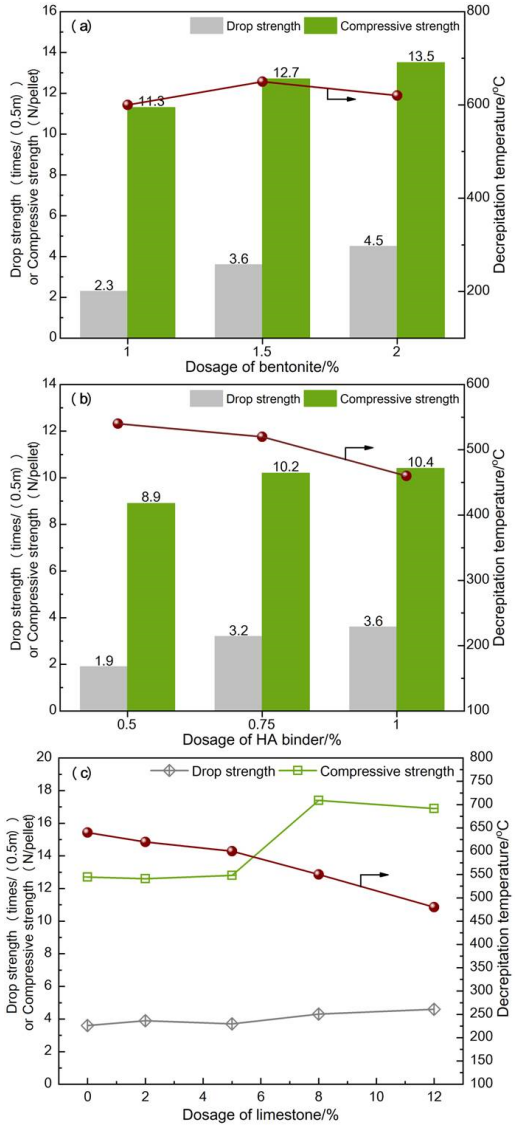

Figure 3. Effects of bentonite (**a**), HA binder (**b**), and limestone dosage (**c**) on the green balls' properties.

As can be seen from Figure 3a, to produce qualified green balls, the minimum requirement for bentonite dosage is 1.5%. Its drop strength and compressive strength reach 3.6 times/0.5 m and 12.7 N/pellet, respectively. These two indexes further increase to 4.5 and 13.5 with bentonite dosage rising to 2.0%. However, bentonite dosage does not show any apparent impact on the decrepitation temperature of green balls. It always remains higher than 600 °C when bentonite is used as binder. The dosage of binder can be markedly reduced when the HA binder is blended in. Figure 3b shows that qualified green balls with drop strength of 3.2 times/0.5 m and compressive strength of 12.7 N/pellet can be obtained with 0.75% of HA binder (only half the bentonite dosage). The decrepitation temperature drops to 520 °C as compared with bentonite green balls, which can probably be attributed to the decomposition of the organic components in the HA binder [4,8], but it still can meet the standard of green balls. As shown in Figure 3c, 0~12% of limestone blending does not show any negative influence on the drop and compressive strength of green balls based on the 0.75% of HA binder dosage. When the limestone dosage reaches 8.0%, the compressive strength of the green ball reaches the level of 18 N/pellet. The decrepitation temperature of green balls declines notably when more than 5% of limestone is blended in. As shown in Figure 2, limestone with D_{50} of 6.75 μm is much finer than the VTM concentrate. Certain amounts of fine particles in the raw material can improve the density and strength of the green balls, but too much may lead to overly dense structure of balls and, therefore, the decrease in decrepitation temperature.

3.2. Effect of HA Binder on Sintering Characteristic

Figure 4 provides the compressive strength of bentonite, HA, and limestone bound pellets obtained by different preheating/roasting conditions. As the most important index of oxidized pellets, the compressive strength requirement for medium and large blast furnaces is 2000~2500 N/P or higher [15–17].

For the 1.5% bentonite-blended pellet, its compressive strength shows a steady upward trend with the preheating temperature (Figure 4a). The compressive strength of pellets reaches 2512 N/P when preheated at 950 °C, which meets the requirement of the blast furnace. The strength then slightly increases to 2654 N/P as the preheating temperature rises to 1000 °C. Prolongation of the preheating time seems to show a greater impact on the compressive strength, as demonstrated in Figure 4b. To be specific, the compressive strength increases from 2512 N/P to 2722 N/P with the time prolonged from 15 min to 18 min. The increase is more apparent than that caused by temperature rise. Similar change rules are also observed in the preheating of the 0.75% HA-binder-blended pellet.

Differences also exist between the bentonite- and HA-bonded pellets. For the first, the compressive strength of the HA-bonded pellets obtained by the same sintering condition is always lower than that of bentonite-bonded pellets, but it still can reach the level of >2000 N/P. In addition, the HA-bonded pellets require a longer preheating time (18 min, as shown in Figure 4b). This is possibly related to the decomposition of the HA binder during the preheating process. Then, qualified oxidized pellets can be obtained with a roasting temperature $\geq$ 1250 °C and time $\geq$ 8 min both for bentonite- and HA-bonded pellets. Based on the 0.75% of HA binder blending, the compressive strength of sintered pellets peaking at 5% of limestone dosage reaches 2573 N/P (shown in Figure 4e) under the optimized sintering condition (preheating at 950 °C for 15 min and then roasting at 1250 °C for 10 min). The basicity of pellets reaches 0.6 at this point. Limestone addition induces the formation of calcium ferrite ($CaO{\cdot}Fe_2O_3$, a low melting point phase) during the high-temperature sintering process [15,18,19], which helps to improve the strength of the HA pellets. However, excessive low-melting-point substance formation could hinder the transfer of oxygen in pellets, which can obstruct the oxidation and crystallization of the iron oxide phase, and, consequently, lowers the compressive strength of pellets [20].

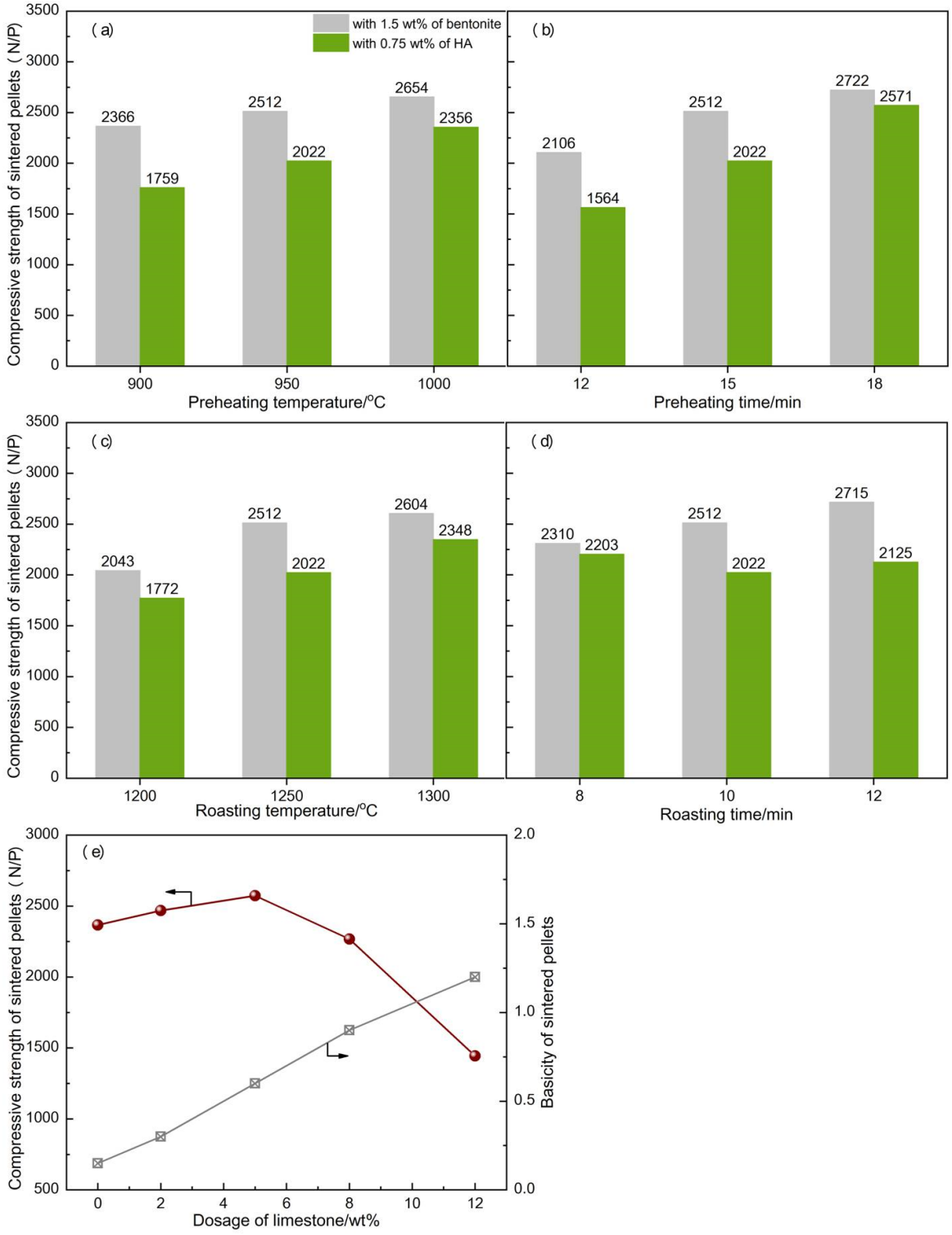

Figure 4. Preheating (**a**,**b**) and roasting (**c**,**d**) properties of bentonite, HA binder, and limestone (**e**) blended pellets.

3.3. Effect of HA Binder on the Phase Structure of Sintered Pellets

From the pelletizing results discussed above, qualified pellets can be prepared by VTM with 1.5% bentonite, 0.75% HA, or 0.75% HA + 5% limestone, respectively. The XRD patterns of these three sintered pellet samples are shown in Figure 5.

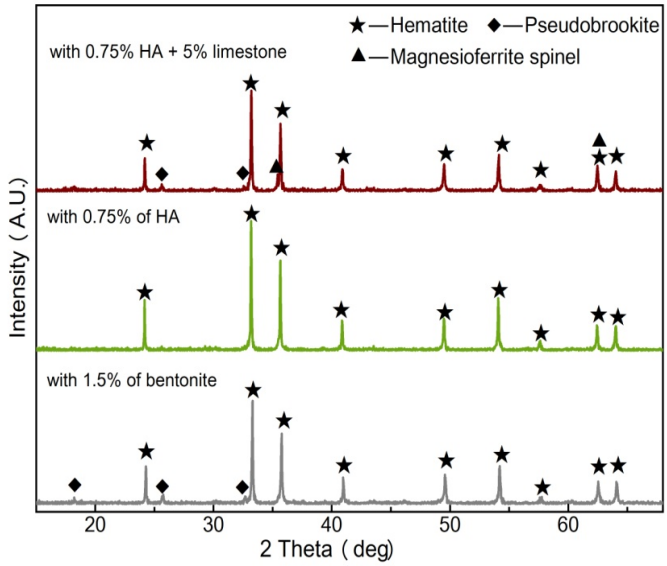

Figure 5. XRD pattern of sintered pellets.

There is no big difference in the phase characteristics among the three pellet samples. Similar to all other oxidized pellets, hematite constitutes their major mineral phase. Beyond that, an extra minor phase (pseudobrookite) is found in bentonite- and limestone-doped pellets. Pseudobrookite, as an iron-containing brookite, is commonly seen in the VTM oxidation process [21,22], and trace magnesioferrite spinel phase is detected only in the limestone-doped fluxed pellets. Magnesioferrite spinel is a common phase during fluxed pellet production. It is always formed by the solid-phase reaction of MgO with hematite or magnetite above 600 °C. The lattice of magnetite could be stabilized with MgO penetrated in [23], which is unfavorable for the oxidation and induration of pellets.

The morphology of the hematite phase in the three sintered pellet samples were observed by an optical microscopy, as shown in Figure 6. In the bentonite-doped pellet (Figure 6a,b), single hematite (bright white, fine grain shape) develops to a relatively complete plate-like state, leaving tiny pores (black, irregular shape) between the interconnected hematite grains. As the strength of the oxidized pellets mainly depends on the crystallization of hematite grains [15], the physical and chemical conditions for hematite upgrowth during the sintering process is especially crucial. However, the crystalline state is visibly poor, with more and bigger pores between the hematite grains in the HA-doped pellet (Figure 6c,d). This explains why the strength of the HA pellets is slightly lower, as shown by the results given in Figure 4. HA pellets always need more sintering time for the crystallization of the hematite grains, but 5% of limestone blending promotes the growth of the hematite grains of HA pellets, as shown in Figure 6e,f. The melting substance formed in limestone-doped pellets could, to some extent, improve the diffusion of hematite grains. We observe that fine grains develop to plump ones (size: 10~20 μm) with full interlocking. Therefore, the induration of HA pellets can be strengthened by proper limestone addition, as the data show in Figure 4e.

The morphology of the pseudobrookite and magnesioferrite spinel phase in the sintered pellet sample were further identified by an SEM equipped with EDS, as presented in Figures 7 and 8, respectively. From the SEM images (cross-section), a symbiotic relationship between the pseudobrookite and hematite can be found. The pseudobrookite phase is needle-like (spot ① in Figure 7), but in fact flake-like in the unbroken pellet. It wraps around the iron oxides (spot ② in Figure 7), which leads to the oxidation of VTM that is more difficult than that of ordinary magnetite.

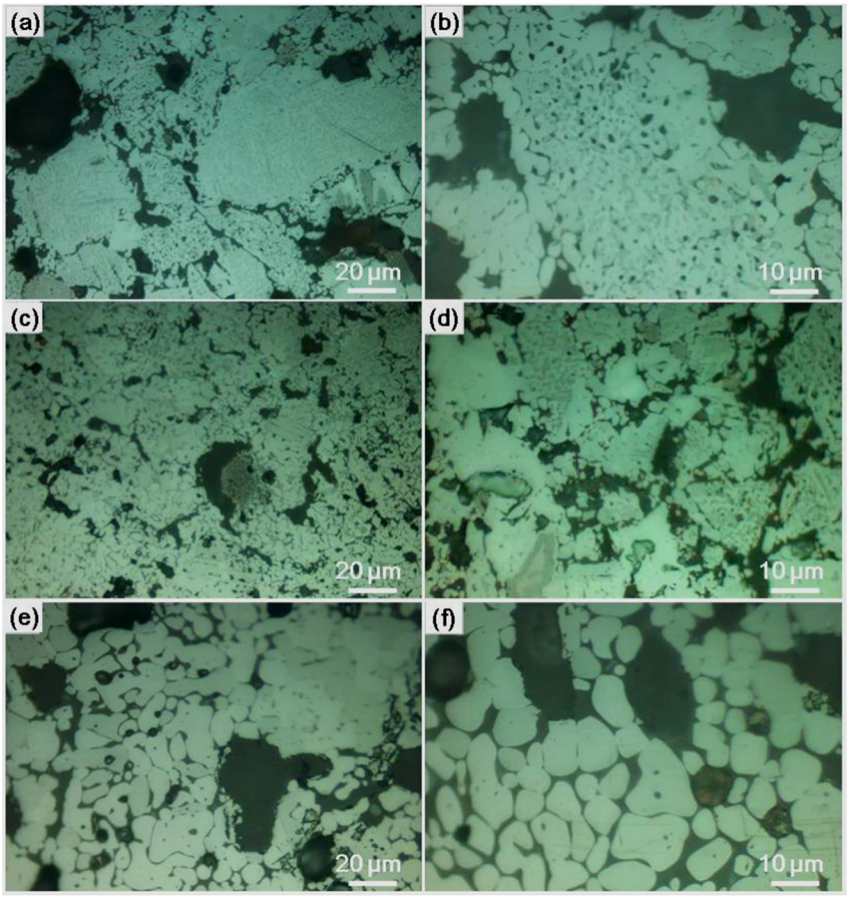

Figure 6. Micrographs of sintered pellet (cross-section) with 1.5% bentonite (**a**,**b**), 0.75% HA (**c**,**d**), and 0.75% HA + 5% limestone (**e**,**f**).

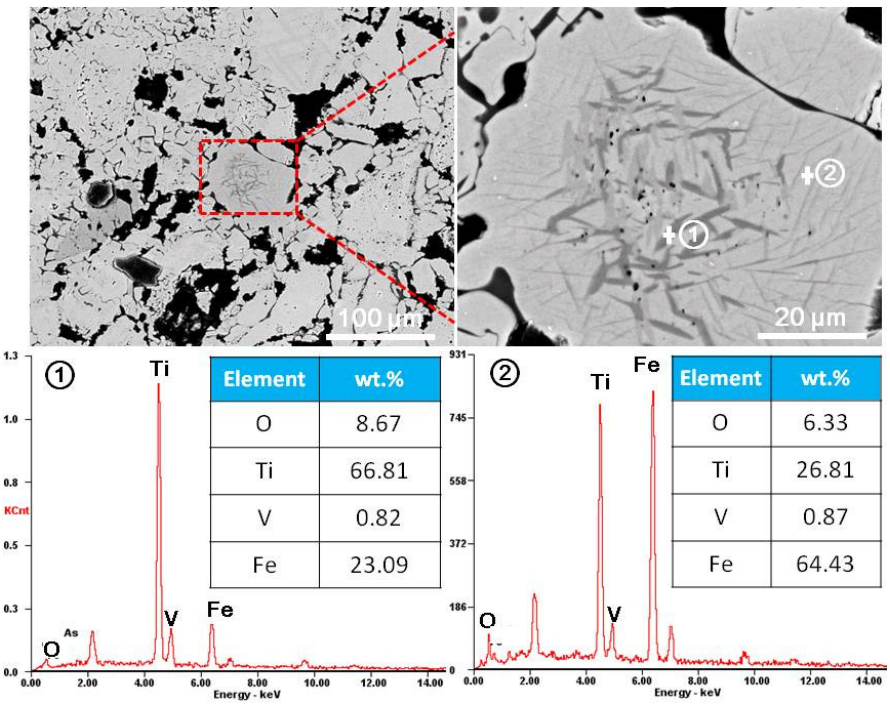

Figure 7. Distribution characteristics of pseudobrookite in the sintered pellets.

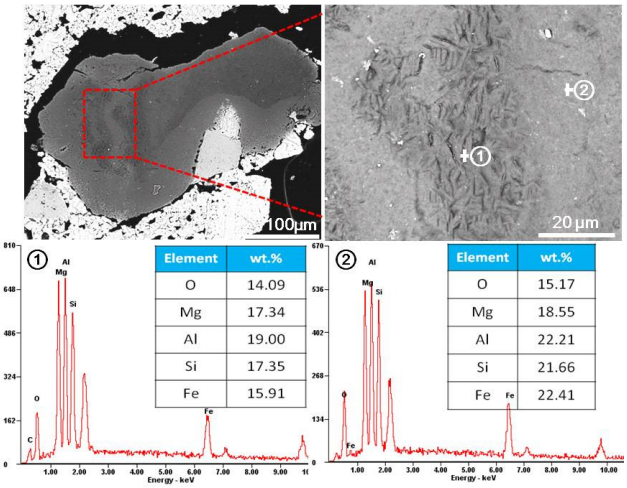

Figure 8. Distribution characteristics of magnesioferrite spinel in the sintered pellets.

The magnesioferrite spinel in a piece shape (dark grey in Figure 8), wraps around other minerals, forming large pores around it. The liquid phase (containing magnesium, aluminum, and silicon components) induces the generation of magnesioferrite spinel phase at high temperatures. Then, it shrinks during the pellet-cooling process, leaving large pores around it. The formation of this structure may cause strength deterioration in the final pellets.

Figure 9 shows the distribution characteristics and symbiotic relationship of each phase. Hematite is the major phase of the final pellets. The well-crystallized hematite grains (bright white, area ② in Figure 9) ensure the necessary strength of the pellets. However, the interconnection state of hematite is cut off when pseudobrookite (light grey, area ① in Figure 9) emerges. This undesirably inhibits the upgrowth of hematite grains. The formation of a connecting neck or inter-solution can be found between the magnesioferrite spinel (dark grey, area ④ in Figure 9) and pseudobrookite phase. However, almost no interconnection forms between the magnesioferrite spinel and hematite. Thus, strengthening the VTM oxidation and regulating the magnesioferrite spinel formation during the sintering process are crucial to improve the induration of HA-bonded pellets.

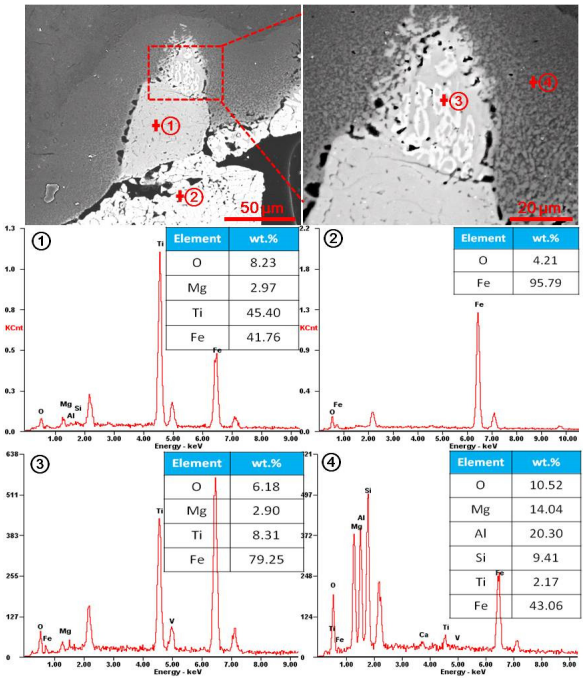

Figure 9. The embedding relationship of each mineral phase in sintered pellet.

4. Conclusions

(1) Qualified oxidized pellets with compressive strength higher than 2000 N/P can be prepared by VTM concentrate with 0.75% of HA binder. The dosage of the binder can be reduced by 50% when HA is used instead of bentonite. The compressive strength of HA pellets can be further improved to higher than 2500 N/P when 5% of limestone is blended in;

(2) For the sintered pellets with HA binder, fine hematite grains crystallize, with more pores embed in. However, 5% of limestone blending drives the fine hematite grains to evolve to a plump interlocking state. The formation of pseudobrookite and magnesioferrite spinel phase during sintering treatment could hinder the crystallization of hematite grains, and cause strength decline in the final pellets.

Author Contributions: Conceptualization, G.L.; methodology, Y.Z.; formal analysis, X.Z.; investigation, Y.Z. and P.C.; data curation, F.M.; writing—original draft preparation, G.L. and Y.Z.; writing—review and editing, L.Y.; project administration, L.Y. All authors have read and agreed to the published version of the manuscript.

Funding: This work was financially supported by the National Natural Science Foundation of China (No. 52274286), and the Natural Science Foundation of Hunan Province (No. 2021JJ40719).

Institutional Review Board Statement: Not applicable.

Informed Consent Statement: Not applicable.

Data Availability Statement: The data presented in this study are available on reasonable request from the corresponding author.

Conflicts of Interest: The authors declare no conflict of interest.

References

1. Wang, H.T.; Zhao, W.; Chu, M.S.; Feng, C.; Liu, Z.G.; Tang, J. Current status and development trends of innovative blast furnace ironmaking technologies aimed to environmental harmony and operation intellectualization. *J. Iron Steel Res. Int.* **2017**, *24*, 751–769. [CrossRef]
2. Wang, Y.J.; Zuo, H.B.; Zhao, J. Recent progress and development of ironmaking in China as of 2019: An overview. *Ironmak. Steelmak.* **2020**, *47*, 640–649. [CrossRef]
3. "China's Pellet Production Will Reach 230 Million Tons in 2022" (Zhonglian Steel United Steel Network, 2022). Available online: https://www.zgltw.cn/m/view.php?aid=40012 (accessed on 26 January 2023).
4. Kawatra, S.K.; Claremboux, V. Iron Ore Pelletization: Part II. Inorganic Binders. *Miner. Process. Extr. Metall. Rev.* **2022**, *43*, 813–832. [CrossRef]
5. Mohamed, O.A.; Shalabi, M.E.H.; El-Hussiny, N.A.; Khedr, M.H.; Mostafa, F. The role of normal and activated bentonite on the pelletization of barite iron ore concentrate and the quality of pellets. *Powder Technol.* **2003**, *130*, 277–282. [CrossRef]
6. Wang, C.; Xu, C.Y.; Liu, Z.J.; Wang, Y.Z.; Wang, R.R.; Ma, L.M. Effect of organic binders on the activation and properties of indurated magnetite pellets. *Int. J. Min. Met. Mater.* **2021**, *28*, 1145–1152. [CrossRef]
7. Zhou, J.A.; Wang, J.; Wang, B.; Ding, B.; Dang, Y.C.; Li, Y.J. The bonding mechanism and effects of sodium ligninsulfonate (SL) in iron ore pelletization. *Metall. Res. Technol.* **2022**, *119*, 303. [CrossRef]
8. Kawatra, S.K.; Claremboux, V. Iron Ore Pelletization: Part I. Fundamentals. *Miner. Process. Extr. Metall. Rev.* **2022**, *43*, 529–544. [CrossRef]
9. Alsaqoor, S.; Borowski, G.; Alahmer, A.; Beithou, N. Using of Adhesives and Binders for Agglomeration of Particle Waste Resources. *Adv. Sci. Technol. Res.* **2022**, *16*, 124–135. [CrossRef]
10. Zhou, Y.L.; Zhang, Y.B.; Li, P.; Li, G.H.; Jiang, T. Comparative study on the adsorption interactions of humic acid onto natural magnetite, hematite and quartz: Effect of initial HA concentration. *Powder Technol.* **2014**, *251*, 1–8. [CrossRef]
11. Zhou, Y.L.; Zhang, Y.B.; Li, G.H.; Wu, Y.D.; Jiang, T. A further study on adsorption interaction of humic acid on natural magnetite, hematite and quartz in iron ore pelletizing process: Effect of the solution pH value. *Powder Technol.* **2015**, *271*, 155–166. [CrossRef]
12. Han, G.H.; Huang, Y.F.; Li, G.H.; Zhang, Y.B.; Jiang, T. Detailed Adsorption Studies of Active Humic Acid Fraction of a New Binder on Iron Ore Particles. *Miner. Process. Extr. Metall. Rev.* **2014**, *35*, 1–14. [CrossRef]
13. Li, W.; Fu, G.Q.; Chu, M.S.; Zhu, M.Y. Investigation of the oxidation induration mechanism of Hongge vanadium titanomagnetite pellets with different Al_2O_3 additions. *Powder Technol.* **2020**, *360*, 555–561. [CrossRef]
14. Fu, G.Q.; Li, W.; Chu, M.S.; Zhu, M.Y. Influence Mechanism of SiO2 on the Oxidation Behavior and Induration Process of Hongge Vanadium Titanomagnetite Pellets. *Metall. Mater. Trans. B* **2020**, *51*, 114–123. [CrossRef]
15. Fu, J.Y.; Jiang, T.; Zhu, D.Q. *Sintering and Pelletizing*; Central South University Press: Changsha, China, 1996; pp. 160–165.

16. Shi, Y.; Zhu, D.Q.; Pan, J.; Guo, Z.Q.; Lu, S.H.; Xu, M.J. Improving hydrogen-rich gas-based shaft furnace direct reduction of fired hematite pellets by modifying basicity. *Powder Technol.* **2022**, *408*, 117782. [CrossRef]
17. Huang, Z.C.; Yi, L.Y.; Jiang, T. Mechanisms of strength decrease in the initial reduction of iron ore oxide pellets. *Powder Technol.* **2012**, *221*, 284–291. [CrossRef]
18. Yi, L.Y.; Huang, Z.C.; Jiang, T.; Zhong, R.H.; Liang, Z.K. Iron ore pellet disintegration mechanism in simulated shaft furnace conditions. *Powder Technol.* **2017**, *317*, 89–94. [CrossRef]
19. Park, T.J.; Choi, J.S.; Min, D.J. In Situ Observation of Crystallization in CaO-Fe_2O_3 System with Different Cooling Rates and Chemical Compositions Using Confocal Laser Scanning Microscope. *Metall. Mater. Trans. B* **2018**, *49*, 2174–2181. [CrossRef]
20. Xiao, Y.Y.; Zhu, K.; Ye, S.X.; Xie, Z.Y.; Zhang, Y.W.; Lu, X.G. Hydrogen on softening-melting and slag forming behavior under the operation of blast furnace with iron coke charging. *Int. J. Hydrogen Energy* **2022**, *47*, 31129–31139. [CrossRef]
21. Gan, M.; Sun, Y.F.; Fan, X.H.; Ji, Z.Y.; Lv, W.; Chen, X.L.; Jiang, T. Preparing high-quality vanadium titano-magnetite pellets for large-scale blast furnaces as ironmaking burden. *Ironmak. Steelmak.* **2020**, *47*, 130–137. [CrossRef]
22. Sui, Y.L.; Guo, Y.F.; Jiang, T.; Qiu, G.Z. Separation and recovery of iron and titanium from oxidized vanadium titano-magnetite by gas-based reduction roasting and magnetic separation. *J. Mater. Res. Technol.* **2019**, *8*, 3036–3043. [CrossRef]
23. Zhu, D.Q.; Chun, T.J.; Pan, J.; Zhang, J.L. Influence of basicity and MgO content on metallurgical performances of Brazilian specularite pellets. *Int. J. Miner. Process.* **2013**, *125*, 51–60. [CrossRef]